

CASE REPORT

A novel COL2A1 mutation causing spondyloepiphyseal dysplasia congenita in a Chinese family

Tangjun Zhou | Xiao Yang | Zhiqian Chen | Yifan Zhou | Xiankun Cao |
Changqing Zhao | Jie Zhao 

Department of Orthopedics, Shanghai Key Laboratory of Orthopedic Implants, Ninth People's Hospital, Shanghai Jiaotong University School of Medicine, Shanghai, China

Correspondence

Jie Zhao, Shanghai Key Laboratory of Orthopedic Implants, Department of Orthopedics, Ninth People's Hospital, Shanghai Jiaotong University School of Medicine, 639 Zhizaoju Road, Shanghai, 200011, China.
Email: profzhaojie@126.com

Funding information

National Natural Science Foundation of China, Grant/Award Number: 81871790

Abstract

Background: Spondyloepiphyseal dysplasia congenita is an autosomal dominant cartilaginous dysplasia characterized by short trunk, abnormal epiphysis, and flattened vertebral body. Skeletal features of SEDC are present at birth and evolve over time. Other features of SEDC include myopia and/or retinal degeneration with retinal detachment and cleft palate. A mutation in the COL2A1 gene located in 12q13.11 is considered as one of the important causes of SEDC. In 2016, Barat-Houari et al. reported a large number of COL2A1 mutations. Among them, a non-synonymous mutation in COL2A1 exon 37, c.2437G>A (p. Gly813Arg), has been reported to cause SEDC in only one patient from France so far.

Methods: We followed up a patient with SEDC phenotype and his family members. The clinical manifestations, physical examination and imaging examination, including X-ray, CT and MRI, were recorded. The whole-exome sequencing was used to detect the patients' genes, and the pathogenic genes were screened out by comparing with many databases.

Results: We report a Chinese patient with SEDC phenotype characterized by short trunk, abnormal epiphysis, flattened vertebral body, narrow intervertebral space, dysplasia of the odontoid process, chicken chest, scoliosis, hip and knee dysplasia, and joint hypertrophy. Gene sequencing analysis showed that the patient had a heterozygous mutation (c.2437G>A; p. Gly813Arg) in the COL2A1 gene. No COL2A1 mutation or SEDC phenotype was observed in his family members. This is the first report of SEDC caused by this mutation in an East Asian family.

Conclusion: This report provides typical clinical, imaging, and genetic evidence for SEDC, confirming that a de novo mutation in the COL2A1 gene, c.2437G>A (p. Gly813Arg), causes SEDC in Chinese population.

KEYWORDS

Chinese population, COL2A1, occipitocervical fusion, odontoid process dysplasia, spondyloepiphyseal dysplasia congenita (SEDC), upper cervical decompression

Tangjun Zhou and Xiao Yang contributed equally to this work.

This is an open access article under the terms of the Creative Commons Attribution-NonCommercial-NoDerivs License, which permits use and distribution in any medium, provided the original work is properly cited, the use is non-commercial and no modifications or adaptations are made.

© 2021 The Authors. *Journal of Clinical Laboratory Analysis* published by Wiley Periodicals LLC

1 | INTRODUCTION

Spondyloepiphyseal dysplasia congenita (SEDC, OMIM 183900) is an autosomal dominant disease. It mainly causes bone lesions and is characterized by short stature, abnormal epiphysis, flat vertebral body, narrow intervertebral space, odontoid dysplasia, scoliosis, hip and knee dysplasia, and joint hypertrophy. This genetic disease is mainly caused by mutations in the *COL2A1* gene.¹ Barat-Houari et al. reported a large database of SEDC-causing *COL2A1* mutations. However, a non-synonymous mutation in *COL2A1* exon 37, c.2437G>A (p. Gly813Arg), has been found to cause SEDC in only one patient from France. This pathogenic mutation leads to substitution of glycine for arginine at amino acid position 813 (p. Gly813Arg) in the A1 chain of type II collagen, causing SEDC.²

Barat-Houari et al. studied *COL2A1* mutations in detail enrolling 136 patients with a skeletal dysplasia phenotype.² However, no specific case of SEDC caused by the non-synonymous mutation in *COL2A1* exon 37, c.2437G>A (p. Gly813Arg), has been reported. Here, we report a new case of SEDC caused by c.2437G>A (p. Gly813Arg) in a Chinese patient. This is the first case of SEDC caused by this mutation in an East Asian patient.

2 | CASE REPORT

Pedigree of the family of the Chinese patient with SEDC is shown in Figure 1. At the age of 41, the proband (II-2) visited our hospital because of progressive numbness in four limbs for 2 months, chest tightness, and shortness of breath for more than 1 month. Based on the medical history, the patient was diagnosed with dwarfism since

his childhood. He was also diagnosed with bilateral hip subluxation more than 10 years ago without treatment. Cholecystectomy was performed at a local hospital 2 months before admission. At the time

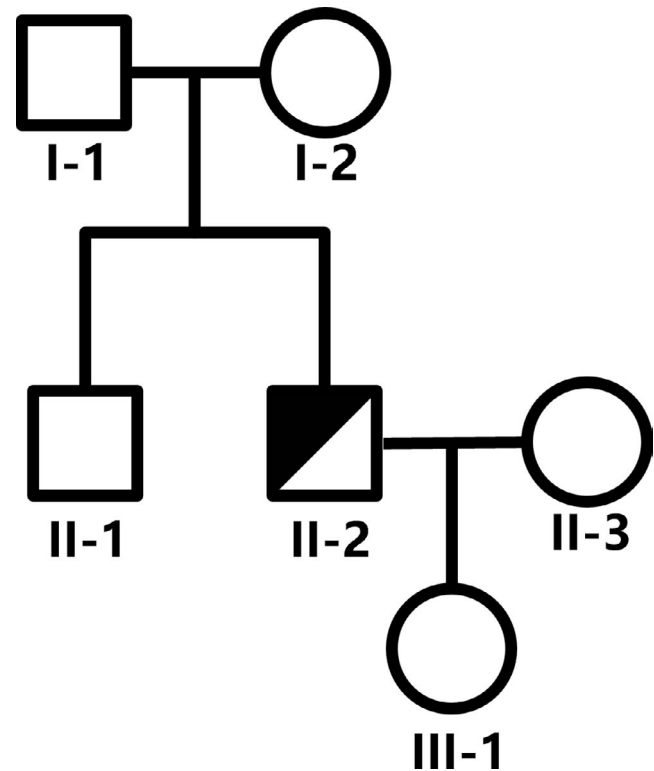


FIGURE 1 Pedigree of the Chinese family with spondyloepiphyseal dysplasia congenita. The proband (II-2) is indicated with the closed symbol

TABLE 1 Physical examination of neurological function pre/post-operation

NR	Pain on left (pre-OP/post-OP)	Tactual sensation on left (pre-OP/post-OP)	Pain on right (pre-OP/post-OP)	Tactual sensation on right (pre-OP/post-OP)
C2	2/2	2/2	2/2	2/2
C3	2/2	2/2	2/2	2/2
C4	2/2	2/2	2/2	2/2
C5	2/2	2/2	2/2	2/2
C6	½	½	½	1/2
C7	1/1	1/1	1/1	1/1
C8	½	½	½	1/2
T1	2/2	2/2	2/2	2/2
T2	2/2	2/2	2/2	2/2
L2	2/2	2/2	2/2	2/2
L3	2/2	2/2	2/2	2/2
L4	2/2	2/2	2/2	2/2
L5	½	½	½	1/2
S1	2/2	2/2	2/2	2/2

Bilateral knee tendon reflex (++++/+++). Bilateral Achilles tendon reflex (++++/+++). Clonus of left ankle (+/-). Bilateral Hoffmann sign (-). Bilateral Babinski sign (-). Muscle strength of four limbs (V).

OP means operation.

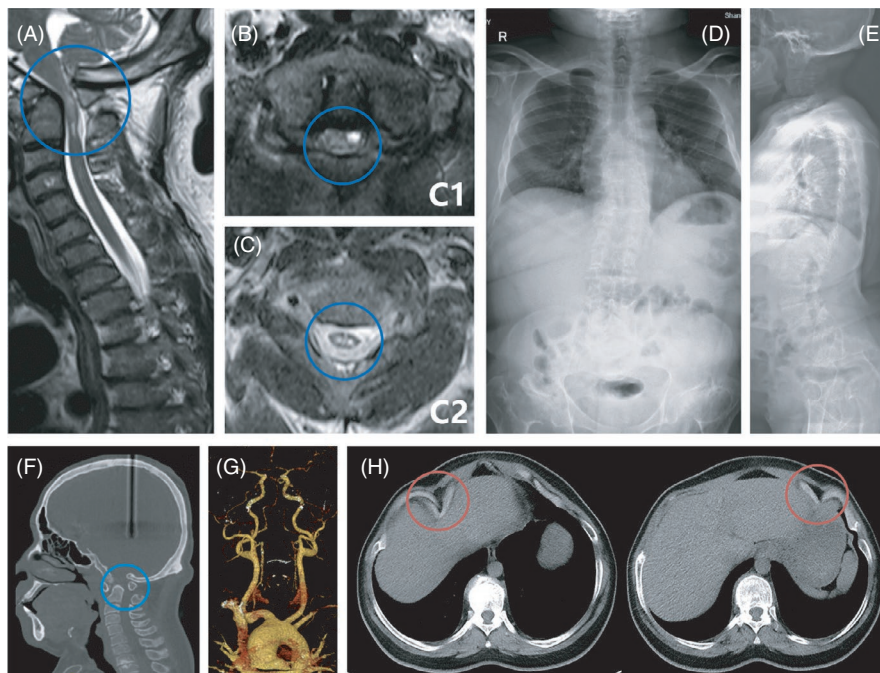


FIGURE 2 Imaging examination findings of the proband (II-2) at the age of 41. A, Sagittal magnetic resonance imaging (MRI) of the cervical spine. B, Transection MRI of C1. C, MRI revealing high cord signals at C2. MRI (A-C) show high signal intensity in the cervical spinal cord, dysplasia of the odontoid process, basilar invagination, and upper cervical spinal canal stenosis, which is marked by blue circle. D, Whole spine X-ray in anteroposterior view. E, Whole spine X-ray in lateral view. Radiographs show flat vertebral body, narrow intervertebral space, irregular endplates, scoliosis, and hip and knee dysplasia. F, Reconstruction of computed tomography (CT) scan shows upper cervical spinal canal stenosis marked by blue circle. G, Reconstruction of CT angiography showing no obvious vertebral artery stenosis. H, Chest CT shows chest compression caused by rib invagination

of admission, the patient's height was 121 cm; he had short fingers and toes as well as facet hypertrophy. In addition to short stature, the most direct causes of the patient's admission were numbness in hands and feet, a decrease in flexibility of both hands, and an unstable walking that began 2 months before the admission. At the same time, he also experienced chest tightness, shortness of breath, and aggravation of dyspnea that started one month before the admission. Dyspnea is characterized by intermittent attacks and progressive aggravation, even when the patient is not physically active. The above-mentioned symptoms were also accompanied by intermittent traction pain below costal arch, binocular pain, and blurred vision. Although the conservative treatment started half a month after the onset of symptoms, the symptoms gradually worsened.

Physical examination showed hypoesthesia in the areas innervated by nerve from C6, C7, C8, and L5, hyperreflexia of bilateral knee tendon and bilateral Achilles tendon, positive left ankle clonus, negative bilateral Hoffmann sign, negative bilateral Babinski sign, and grade V muscle strength in all four limbs (Table 1).

Figure 2 shows imaging examination findings. Magnetic resonance imaging (MRI) revealed high signal intensity in the cervical spinal cord. The combination of computed tomography (CT) and MRI led to a comprehensive diagnosis of odontoid process dysplasia, basilar invagination, and upper cervical spinal canal stenosis in the patient. Whole spine X-rays in anteroposterior view showed flat vertebral body, narrow intervertebral space, irregular endplates,

scoliosis, and hip and knee dysplasia. Reconstruction of the vertebral artery from CT angiography showed no obvious vertebral artery stenosis, excluding the diagnosis of vertebral artery type cervical spondylosis. Chest CT revealed thoracic deformity and chest compression caused by rib invagination, which is another symptom of SEDC; the patient experienced chest tightness may be partly due to thoracic deformity.

After communicating with the patients and their families and obtaining informed consent, we collected saliva from the patient and his family. NanoDrop (iGeneTech, Beijing China) was used to detect the concentration and purity of DNA extracted from saliva. Agarose gel electrophoresis was used to detect the degree of DNA degradation and any RNA and protein contamination. The Qubit system (iGeneTech, Beijing China) was used to quantify DNA concentration accurately, and 250 ng of DNA samples was used for whole-exome sequencing by iGeneTech in Beijing, China. After sequencing, we analyzed the exome aggregation consortium database, genome aggregation database, and International Cancer Genome Consortium to screen the available genes. We also used bioinformatics approaches to analyze harmful mutations. The quality control system³⁻⁶ for identifying the candidate variants is shown in Figure 3 and Table 2.

The results of whole-exome sequencing are presented in Table 3. A single-nucleotide polymorphism in the COL2A1 gene with a G to A transition at position 2437, which results in substitution of glycine for arginine at amino acid position 813 (p. Gly813Arg) in the A1

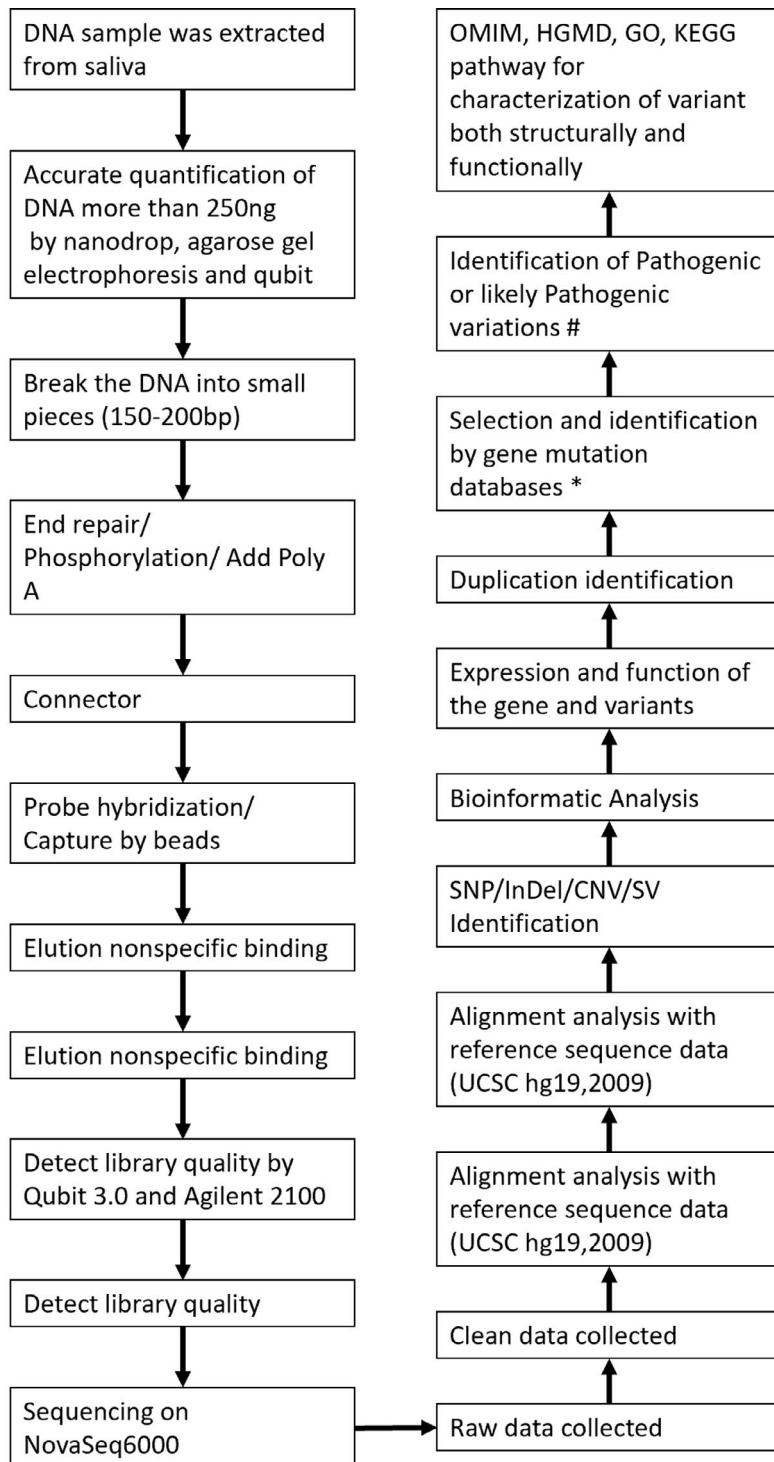


FIGURE 3 Schematic presentation of the quality control system for identifying candidate variants

* Databases include NHLBI-ESP, Exome Aggregation Consortium, Genome Aggregation Database, International Cancer Genome Consortium, ect.

Bioinformatics algorithms include InterVar(automated), dbscSNV ADA SCORE, dbscSNV RF SCORE, SIFT score, Polyphen2 HDIV score, Polyphen2 HVAR score, LRT score, Mutation Taster score, Mutation Assessor score, FATHMM score, CADD raw, fathmm-MKL coding score, GERP++ RS

chain of type II collagen, was identified. Therefore, the patient was diagnosed with SEDC, upper cervical compression. The patient's parents, younger brother, and daughter did not show any skeletal deformity or clinical symptoms.

The patient was then treated by cervical decompression and occipitocervical fusion. The results of postoperative neurological examination are shown in Table 1. The results of postoperative imaging examination are shown in Figure 4. After 6 months of follow-up, the

TABLE 2 Quality control data of whole-exome sequencing

Quality control of raw data	
Raw reads (M)	76.48
Raw bases (Mb)	11548.26
Clean reads (M)	74.53
Clean bases (Mb)	10885.05
QC rate (%)	94.26
Library quality assessment	
Average read length	144
Average base quality	35.4
Average insert size	271.2
Clean bases (Mb)	10885.05
QC rate (%)	94.26
Duplication rate (%)	20.29
Mapped reads (M)	60.27
Accurate mapped bases (Mb)	8579.0
Accurate mapping rate (%)	98.45
Target size	58231156
Target covered size	58164782
Coverage rate (%)	99.89
Target overlapped reads (M)	47.25
Reads capture rate (%)	78.4
Target effective bases (Mb)	5639.62
Bases capture rate (%)	65.74
Target mean depth	96.85
4× coverage rate (%)	99.7
10× coverage rate (%)	99.09
20× coverage rate (%)	97.01
5%× mean depth coverage rate (%)	99.7
20%× mean depth coverage rate (%)	97.29
50%× mean depth coverage rate (%)	81.54
Flank 10%× mean depth coverage rate (%)	13.98

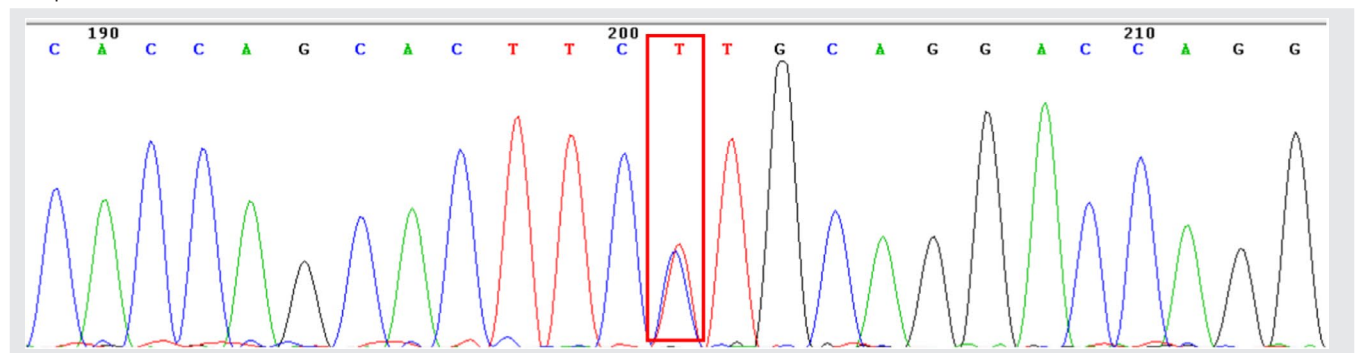
patient's symptoms, such as limb numbness, chest tightness, shortness of breath, unstable walking, and lack of hand flexibility, were significantly relieved. Physical examination showed that the sensory function in the areas innervated by C6, C7, C8, and L5 nerve recovered. Knee reflexes changed from hyperactive to activity, Achilles tendon reflexes from hyperactive to normal, and ankle clonus changed from positive to negative.

3 | DISCUSSION

We report the pedigree of a Chinese family with SEDC. There was only one patient with SEDC in the family. This is the first report on SEDC caused by c.2437G>A in East Asians. Whole-exome sequencing data of the patient's family clearly indicated that the disease was caused by a de novo mutation in the COL2A1 gene (Figure 1). The mutation in the COL2A1 gene was identified as c.2437G>A, indicating that the mutation was autosomal dominant. Only one patient from France with SEDC caused by this mutation was reported previously.² The previous study did not report clear imaging data; only a few clinical and imaging descriptions were available. Therefore, it was not possible to compare our results with those from the previous study. The SEDC phenotype of our patient was very clear. The main clinical manifestations of SEDC in our patient, such as short stature, abnormal epiphysis, chicken chest, vertebral body flattening, intervertebral space narrowing, odontoid dysplasia, skull base depression, scoliosis, hip and knee dysplasia, and joint hypertrophy, are shown in Figure 2. Due to the abnormal development of the odontoid process and skull base, the upper cervical spinal canal was narrowed, leading to nerve compression. Preoperative MRI showed a high signal in the medulla, indicating serious nerve compression and nerve degeneration. These observations were combined with the symptoms and signs

TABLE 3 The result of gene sequencing of the patient

HGVS name	Mutation type	Variant location	Gene type	Protein change
NM_001844.4: c. 2437G>A	SNP	Exon 37	Heterozygote	NP_001835.3 p. Gly813Arg
NM_001844.4 CDS start	Ref: TGGTCCTGCA G GAAGTGCTGG Mutation: TGGTCCTGCA A GAAGTGCTGG			
NC_000012.11 Seq start	Ref: CCAGCACTTC C TGCAGGACCA Mutation: CCAGCACTTC T TGCAGGACCA			



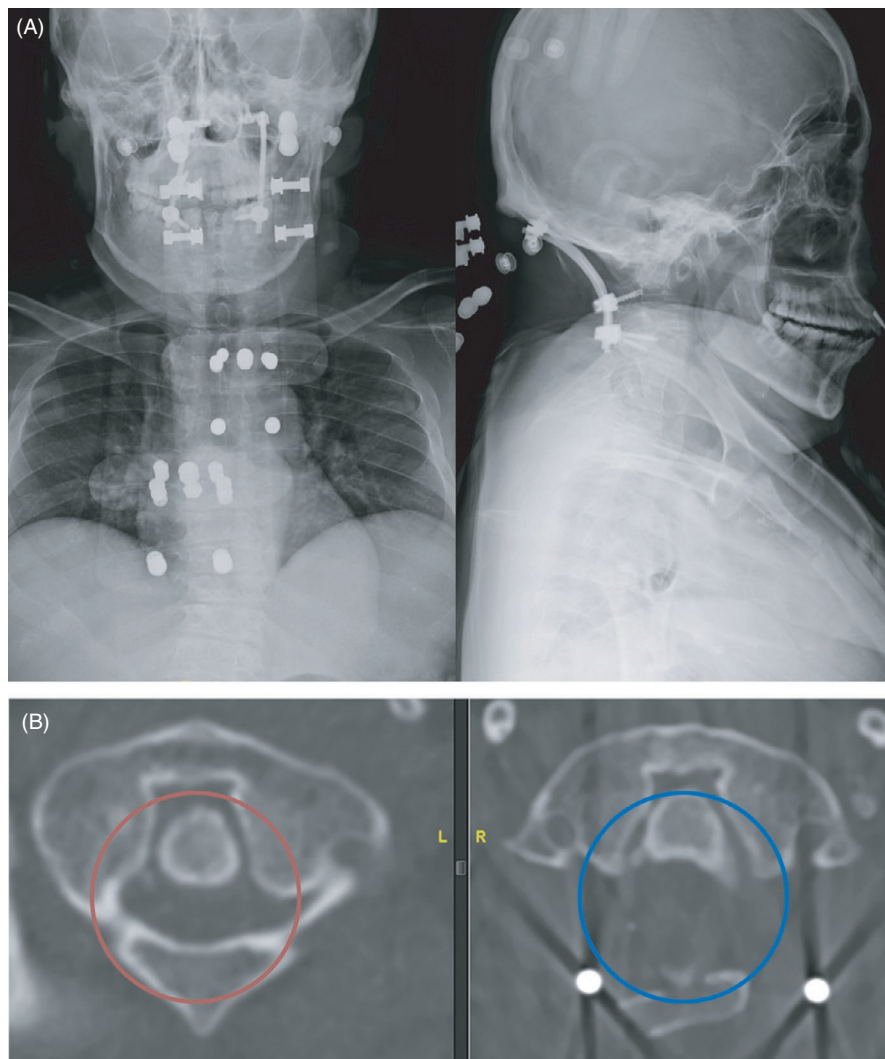


FIGURE 4 A, Anteroposterior and lateral cervical spine X-rays after cervical decompression and occipitocervical fusion. B, Preoperative computed tomography (CT) scan showing upper cervical spinal canal stenosis (red circle). Postoperative CT scan showing the total relief of stenosis (blue circle)

of upper motor neuron dysfunction, such as numbness of limbs, chest banding sensation, dyspnea, unstable walking, and adverse movement of hands. Upper cervical nerve compression secondary to SEDC was definitively diagnosed and treated by cervical decompression and occipitocervical fusion. The patient recovered well after the operation, and he was able to perform light physical labor 6 months postoperatively. One year after the operation, the symptoms of chest tightness and shortness of breath were significantly relieved although there were still residual discomforts. We speculate that the symptoms of chest tightness may be partly due to thorax deformity, and not entirely due to nerve compression. The patient still had hip joint subluxation, knee joint degeneration, and other problems. However, they did not cause symptoms and did not affect the quality of life during follow-up.

In our case, we found that the mutation results in substitution of glycine for arginine at amino acid position 813 (p. Gly813Arg) in the triple helix region of type II collagen, which is very rare among *COL2A1* mutations.² *COL2A1* encodes for type II collagen, the most important and abundant extracellular matrix protein in epiphysis cartilage. It is closely related to the development and maturation of chondrocytes, synthesis and catabolism of extracellular matrix, and

cartilage ossification.² In mice carrying a *COL2A1* mutation, which eventually lead to a change in the structure of reticular cartilage, reduction of subchondral bone volume and retardation of bone growth are observed. The phenotype of mice carrying a *COL2A1* mutation was similar to that of SEDC patients.⁷ Therefore, SEDC caused by a *COL2A1* mutation often starts from the pathological changes of the epiphysis and articular cartilage. Most SEDC patients undergo hip joint and knee joint replacement because of premature degeneration of cartilage.⁸ Dysplasia of the upper cervical spine causes severe problems associated with upper cervical nerve compression,⁹ similar to those observed in this case. The high level of nerve compression-associated SEDC depresses the respiratory and circulatory centers, and the disease becomes life-threatening. Therefore, surgical treatment in the early stage is more beneficial when neurological symptoms are mild than that in later stage of the disease. In this case, the patient had severe dyspnea; most of the symptoms were relieved after the operation.

Therefore, clinical evaluation should start from childhood to ensure early diagnosis and treatment. As far as the current technology is concerned, early diagnosis and early intervention can be achieved. The CRISPR/cas9 gene editing technology was used in iPSC cells to

study the pathogenesis of SEDC and gene rescue of *COL2A1* mutation.¹⁰ However, further basic research is needed. In addition, we plan to conduct a retrospective case-control study on SEDC including the diagnosis of SEDC, genetic and bioinformatic analyses, and surgical or non-surgical treatment, in order to advance the clinical research on the disease.

ACKNOWLEDGEMENTS

This study relies on the National Natural Science Foundation of China (81871790).

DATA AVAILABILITY STATEMENT

All data and materials included in this study are available upon request by contact with the corresponding author.

ORCID

Jie Zhao  <https://orcid.org/0000-0003-1000-5641>

REFERENCES

- Nenna R, Turchetti A, Mastrogiorgio G, Midulla F. *COL2A1* gene mutations: mechanisms of spondyloepiphyseal dysplasia congenita. *Appl Clin Genet*. 2019;12:235-238.
- Barat-Houari M, Sarrabay G, Gatinois V, et al. Mutation update for *COL2A1* gene variants associated with type II collagenopathies. *Hum Mutat*. 2016;37(1):7-15.
- Dai Y, Liang S, Dong X, et al. Whole exome sequencing identified a novel DAG1 mutation in a patient with rare, mild and late age of onset muscular dystrophy-dystroglycanopathy. *J Cell Mol Med*. 2019;23(2):811-818.
- Han P, Wei G, Cai K, et al. Identification and functional characterization of mutations in *LPL* gene causing severe hypertriglyceridaemia and acute pancreatitis. *J Cell Mol Med*. 2020;24(2):1286-1299.
- Zhang R, Chen S, Han P, et al. Whole exome sequencing identified a homozygous novel variant in *CEP290* gene causes Meckel syndrome. *J Cell Mol Med*. 2020;24(2):1906-1916.
- Zheng Y, Xu J, Liang S, Lin D, Banerjee S. Whole exome sequencing identified a novel heterozygous mutation in *HMBS* gene in a Chinese patient with acute intermittent porphyria with rare type of mild anemia. *Front Genet*. 2018;9:129.
- Donahue LR, Chang B, Mohan S, et al. A missense mutation in the mouse *Col2a1* gene causes spondyloepiphyseal dysplasia congenita, hearing loss, and retinoschisis. *J Bone Miner Res*. 2003;18(9):1612-1621.
- Gregersen PA, and Savarirayan R. 1993. Type II Collagen Disorders Overview. In *GeneReviews*(R), edited by Adam MP, et al. Seattle, WA: University of Washington.1-23.
- Miyoshi K, Nakamura K, Haga N, Mikami Y. Surgical treatment for atlantoaxial subluxation with myelopathy in spondyloepiphyseal dysplasia congenita. *Spine (Phila Pa 1976)*, 2004; 29(21): E488-E491.
- Lilianty J, Nur Patria Y, Stanley EG, Elefanty AG, Bateman JF, Lamande SR. Generation of a heterozygous *COL2A1* (p. R989C) spondyloepiphyseal dysplasia congenita mutation iPSC line, MCRli001-B, using CRISPR/Cas9 gene editing. *Stem Cell Res*. 2020;45:101843.

How to cite this article: Zhou T, Yang X, Chen Z, et al. A novel *COL2A1* mutation causing spondyloepiphyseal dysplasia congenita in a Chinese family. *J Clin Lab Anal*. 2021;35:e23728. <https://doi.org/10.1002/jcla.23728>